Journal of Molecular Catalysis A: Chemical 395 (2014) 392–397

Contents lists available at ScienceDirect

Journal of Molecular Catalysis A: Chemical

journal homepage: www.elsevier.com/locate/molcata

Gas-phase hydrogenation of maleic anhydride to γ-butyrolactone over Cu-CeO_2-Al_2O_3 catalyst at atmospheric pressure: Effects of the residual sodium and water in the catalyst precursor

Yang Yu, Wangcheng Zhan*, Yun Guo, Guanzhong Lu, Souheila Adjimi, Yanglong Guo*

Key Laboratory for Advanced Materials, Research Institute of Industrial Catalysis, East China University of Science and Technology, Shanghai 200237, PR China

ARTICLE INFO

Article history:
Received 10 July 2014
Received in revised form 30 August 2014
Accepted 1 September 2014
Available online 10 September 2014

Keywords:
Maleic anhydride
γ-Butyrolactone
Gas-phase hydrogenation
Cu-CeO_2-Al_2O_3 catalyst
Residual sodium

ABSTRACT

Cu-CeO_2-Al_2O_3 catalysts were prepared by the co-precipitation method with different washing operations during the preparation process for the purpose of controlling the contents of the residual sodium and water in the catalyst precursors. Cu-CeO_2-Al_2O_3 catalysts were characterized by ICP-AES, XRD, SEM, nitrogen sorption, N_2O chemisorption, Raman spectroscopy and H_2-TPR. Effects of the residual sodium and water in the catalyst precursor on the catalytic performance of Cu-CeO_2-Al_2O_3 catalyst for gas-phase hydrogenation of maleic anhydride to γ-butyrolactone at atmospheric pressure, and the structure–activity relationships were investigated. The results show that the residual water and sodium in the form of Na_2CO_3 in the catalyst precursor lead to a decrease in Cu dispersion and Cu surface area, which is disadvantageous to the catalytic performance and stability. Washing step of the residual sodium in the catalyst precursor with the deionized water and then removing step of the residual water using azeotropy distillation shows a great improvement in the stability of Cu-CeO_2-Al_2O_3 catalyst, in which 100% of conversion of maleic anhydride and 100% of selectivity to γ-butyrolactone were maintained for 12 h.

1. Introduction

Direct catalytic hydrogenation of maleic anhydride (MA), as one of the most competitive processes for producing γ-butyrolactone (GBL), has evoked increasing attentions not only due to the widespread applications of GBL as the intermediates for synthesizing pyrrolidone [1,2] and as the cell electrolyte instead of the strong corrosive liquid acid [3,4], but also due to the inexpensive raw material of MA and the simple process. Direct catalytic hydrogenation of MA to GBL includes gas-phase and liquid-phase hydrogenation in terms of the physical state of MA in the reaction process. Liquid-phase hydrogenation preferably employs noble metal catalysts, such as Pd-Sn/SiO_2 [5], Pd/SiO_2 [6] and $RuCl_2(TPP)_3$ [7], in which a high reaction pressure is indispensable. Nevertheless, the yield of GBL is not high enough. In contrast, gas-phase hydrogenation has the advantages of lower reaction pressure, readily continuous production and inexpensive transition metal catalysts, such as Cu-ZnO-MgO-Cr_2O_3 [8], Cu-ZnO-CdO-Cr_2O_3 [9], Cu-ZnO-Al_2O_3 [10], Cu-ZnO-TiO_2 [11], Cu-ZnO-CeO_2 [12], Cu-ZnO-ZrO_2 [13], Cu-ZnO-SiO_2 [14], Cu-CeO_2-Al_2O_3 [15], Ni or Co/SiO_2 [16] and Ni/SiO_2-Al_2O_3 or H-BEA [17,18], in which Cu-based catalysts excel other transition metal catalysts in terms of the catalytic performance.

A large majority of Cu-based catalysts were prepared by the conventional precipitation method using Na_2CO_3 or $NaHCO_3$ aqueous solution as precipitating agent. The residual sodium in the catalyst precursor can lead to variation of the physiochemical properties of the catalyst, and therefore influences its catalytic performance [19,20]. Moreover, in the process of conventional drying in air, the residual water in the catalyst precursor can also contribute to evolution of the physiochemical properties of the catalyst to some extent [21]. For instance, the removal of water during drying process can lead to collapse of the original network structure of the catalyst precursor and agglomeration of the precipitated small particles. Washing with the absolute ethanol can reduce the negative effect of the residual water on the catalysts to a certain extent by substitution of lower-surface-tension ethanol for water [22]. Furthermore, the supercritical fluid drying [23,24] and the azeotropy distillation drying [25] have been proposed to be effective solutions, in which the supercritical fluid drying is expensive and hazardous

* Corresponding authors. Tel.: +86 21 64252923; fax: +86 21 64252923.
E-mail addresses: zhanwc@ecust.edu.cn (W. Zhan), ylguo@ecust.edu.cn (Y. Guo).

http://dx.doi.org/10.1016/j.molcata.2014.09.001
1381-1169/

[26]. In contrast, the azeotropy distillation drying is a promising alternative because of the convenient operation and the recycling characteristic of organic solvent used.

In our previous work [15], Cu-CeO_2-Al_2O_3 catalyst has showed an excellent activity and selectivity for gas-phase hydrogenation of MA to GBL (GHMG) at atmospheric pressure, however its stability still needs to be further improved. In this work, effects of the residual sodium and water in the catalyst precursor on the catalytic performance and stability of Cu-CeO_2-Al_2O_3 catalyst for GHMG at atmospheric pressure, and the structure–activity relationships were investigated.

2. Experimental

2.1. Preparation of catalyst

Cu-CeO_2-Al_2O_3 catalyst (Cu:Ce:Al = 3:6:10, molar ratio) was prepared by the co-precipitation method, described in our previous work [15], in which the aqueous solution of nitrates served as the metal precursor and 1.0 mol L^{-1} of Na_2CO_3 aqueous solution served as the precipitating agent. The resultant precipitate was divided equally into six samples by weight. The sample without any washing operation was labeled as w0, and the other three samples were washed two, four and eight times by centrifugation using the isopyknic deionized water at 70 °C and labeled as w2, w4 and w8, respectively. The residual two samples were washed eight times using the isopyknic deionized water at 70 °C and then followed by deep dehydration with two different methods. One sample was washed two times using absolute ethanol and labeled as w8a2. Another sample was treated using the azeotropy distillation drying in a heterogeneous azeotropy distillation apparatus [22] and labeled as w8ba. In a typical experiment, the sample was mixed with 100 mL of benzene and then kept at 75–81 °C under stirring in oil bath, in which the residual water in the sample and benzene can be co-evaporated. The evaporated water was collected in water trap and the evaporated benzene was refluxed by condenser until the constant water content in water trap. Finally, the benzene was evacuated from the flask by the reduced pressure distillation and the powder was left in the flask. All resultant samples by the above-mentioned different washing operations were designated as the catalyst precursors. All catalyst precursors were then dried overnight at 120 °C, and calcined at 550 °C for 3 h and 650 °C for 3 h in air successively to obtain the as-prepared catalysts. The as-prepared catalysts were pressed and then crushed into 20–40 mesh particles before evaluation of their catalytic performance.

2.2. Gas-phase hydrogenation of maleic anhydride

Gas-phase hydrogenation of maleic anhydride to γ-butyrolactone (GHMG) over Cu-CeO_2-Al_2O_3 catalyst was carried out under atmospheric pressure in a quartz tubular fixed-bed reactor (13 mm I.D., 650 mm L.). In a bottom-up sequence, the reactor was packed with 1 mL of quartz sand pretreated at 600 °C in air, 6 mL of catalyst (height = 45 mm) and then 15 mL of pretreated quartz sand for the complete gasification of raw material (MA dissolved in GBL, 20 wt.%). The catalyst was reduced in situ by 60 mL min^{-1} of 5 vol.% H_2/N_2 at 380 °C for 7 h (designated as the fresh catalyst). Then the temperature was decreased until 240 °C, and the reactor was fed by 30 mL min^{-1} of H_2 and 0.2 h^{-1} of LHSV of raw material. The products were collected in the conical beakers cooled by ice-bath at the interval of 1 h and analyzed by Perkin-Elmer Clarus 500 gas chromatograph equipped with a FID detector and a SE-54 capillary column (25 m × 0.32 mm × 1.0 μm). Both temperatures of injector and detector were kept at 220 °C, and the temperature of column oven was kept at 100 °C for 1 min and then increased programmedly from 100 °C to 120 °C with a heating ramp of 5 °C min^{-1}.

The conversion of MA and the selectivity to GBL were calculated as follows:

$$\text{Conversion of MA} = (n_{MA0} - n_{MA})/n_{MA0} \times 100\%$$

$$\text{Selectivity to GBL} = (n_{GBL} - n_{GBL0})/(n_{MA0} - n_{MA}) \times 100\%$$

n_{MA0} and n_{GBL0} represented the molar amount of MA and the molar amount of GBL in the raw material of 20 wt.% MA dissolved in GBL, respectively. n_{MA} and n_{GBL} represented the molar amount of MA and the molar amount of GBL in the products after MA hydrogenation, respectively.

2.3. Characterization of catalyst

The chemical compositions of the as-prepared catalysts were determined by inductively coupled plasma atomic emission spectroscopy (ICP-AES) using a TJA IRIS ADVANTAG 1000 instrument. The powder XRD patterns were recorded on a Bruker AXS D8 Focus diffractometer with a CuKα radiation (λ = 0.15406 nm) operated at 40 kV × 40 mA, and the diffraction patterns were taken in the range of $10° < 2\theta < 80°$ at the scanning rate of 6° min^{-1}. SEM images were recorded on a JEOL JSM-6360LV scanning electron microscope. The specific surface area was measured by nitrogen sorption at −196 °C with BET method on a NOVA 4200e surface area and pore size analyzer. The Cu surface area (S_{Cu}) and dispersion (D_{Cu} = exposed Cu atoms/total Cu atoms) of the fresh Cu-CeO_2-Al_2O_3 catalysts were measured by N_2O chemisorption at 60 °C assuming a molar stoichiometry of Cu:N_2O = 2 and a surface atomic density of 1.46×10^{19} Cu atoms m^{-2} [27]. Raman spectra were obtained on a Renishaw inVia Reflex Raman microscope with a CCD detector and the excitation wavelength of 785 nm. Raman spectra were recorded at 2 cm^{-1} of increment in the range of 100–1000 cm^{-1}. H_2-TPR was carried out in a conventional flow system equipment with a TCD detector. 50 mg of sample was heated programmedly from room temperature until 850 °C with a heating ramp of 10 °C min^{-1} in the atmosphere of 30 mL min^{-1} of 5 vol. % H_2/N_2.

3. Results and discussion

3.1. Catalytic performance for gas-phase hydrogenation of MA

The catalytic performances of Cu-CeO_2-Al_2O_3 catalysts for GHMG at atmospheric pressure are shown in Fig. 1. As shown in Fig. 1, Na-rich w0 catalyst exhibited the lowest initial catalytic performance with 86.3% of conversion of MA and 78.6% of selectivity to GBL, while the corresponding values increased to 91.2% and 88.8% respectively over w2 catalyst with relatively low sodium content. Furthermore, both the conversion of MA and the selectivity to GBL could reach 100% over w4 and w8 catalysts. According to ICP-AES analysis shown in Table 1, the sodium contents of the as-prepared w0, w2, w4 and w8 catalysts were 6.2 wt.%, 1.5 wt.%, 0.25 wt.% and 0.18 wt.%, respectively. These results obviously indicate that the residual sodium in the catalysts is adverse to the initial catalytic performance of Cu-CeO_2-Al_2O_3 catalysts for GHMG. The negative effect of the residual sodium in Cu-based catalyst on its catalytic performance for methanol synthesis from CO_2 hydrogenation was also observed [19]. As shown in Table 1 and Fig. 1, three catalysts of w8, w8a2 and w8ba, with the same sodium content and the different water content in the precipitate before drying, showed excellent initial catalytic performances with 100% of conversion of MA and 100% of selectivity to GBL, but the catalytic stability of Cu-CeO_2-Al_2O_3 catalysts for GHMG was much different and followed

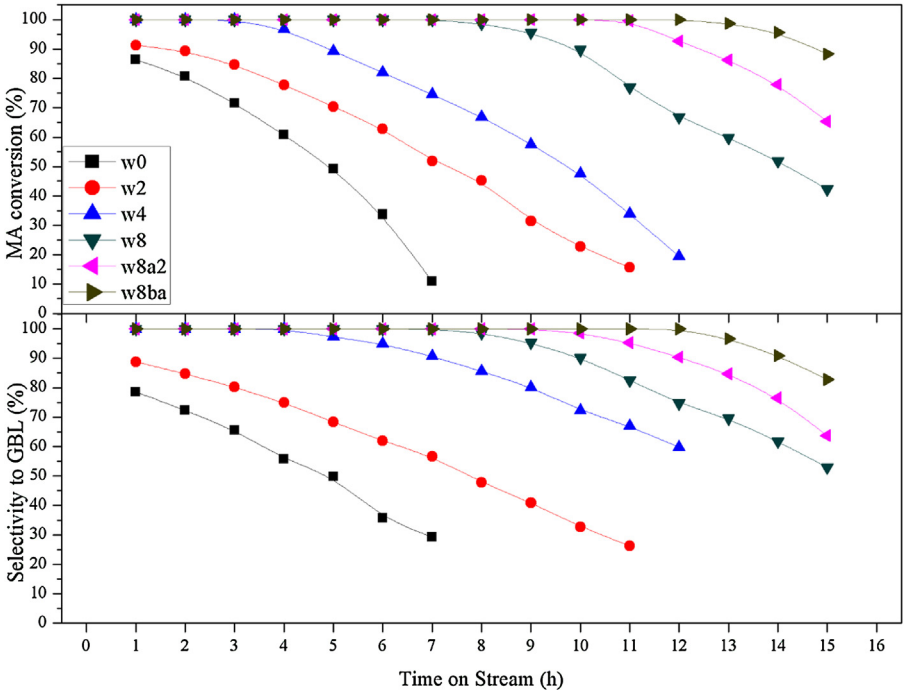

Fig. 1. The catalytic performances of Cu-CeO_2-Al_2O_3 catalysts with different contents of sodium and water in the catalyst precursors for gas-phase hydrogenation of MA to GBL at atmospheric pressure.

an order of w8ba with H_2O of 1.6 wt.% in the precipitate > w8a2 with H_2O of 25.4 wt.% > w8 with H_2O of 56.9 wt.%. For example, 100% of conversion of MA and 100% of selectivity to GBL were maintained for 12 h over w8ba catalyst, but the conversion of MA and the selectivity to GBL decreased to 66.8% and 74.7% over w8 catalyst after reaction for 12 h, respectively, due to the formation of the by-product of succinic anhydride [15], which indicates that the difference in the catalytic performance of the three catalysts of w8, w8a2 and w8ba for GHMG results from the different water content in their precursors. Therefore the residual sodium and water in the catalyst precursors are disadvantageous to the catalytic performances and stabilities of Cu-CeO_2-Al_2O_3 catalysts for GHMG.

3.2. Characterization of Cu-CeO_2-Al_2O_3 catalyst

3.2.1. XRD

Fig. 2 shows XRD patterns of the as-prepared Cu-CeO_2-Al_2O_3 catalysts with different contents of sodium and water in the catalyst precursors. As shown in Fig. 2, the characteristic diffraction peaks of CeO_2 (PDF# 34-0394) were observed in all as-prepared Cu-CeO_2-Al_2O_3 catalysts. However, the characteristic diffraction peaks of CuO (PDF# 65-2309) were only identified in the as-prepared

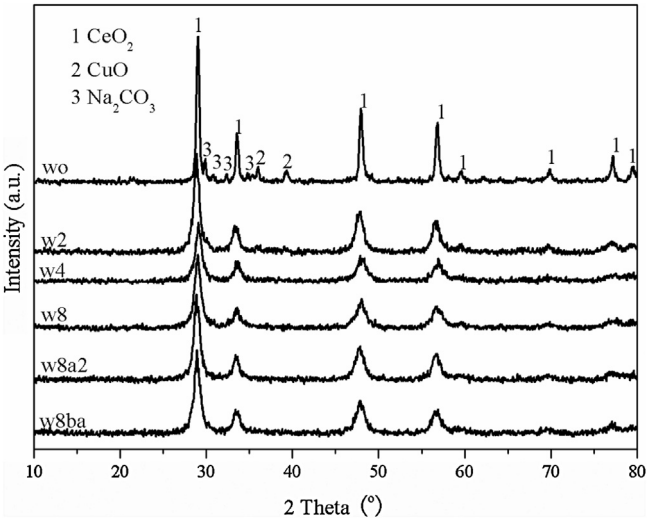

Fig. 2. XRD patterns of the as-prepared Cu-CeO_2-Al_2O_3 catalysts.

Table 1
The physiochemical properties of Cu-CeO_2-Al_2O_3 catalysts with different contents of sodium and water in the catalyst precursors.

Catalysts	Water content (wt.%)[a]	Sodium content (wt.%)[b]	S_{BET} ($m^2\ g^{-1}$)[c]	S_{Cu} ($m^2\ g^{-1}$)[d]	Cu dispersion (%)[d]	Cu particle size (nm)[e]
w0	55.6	6.20	13.5	1.2	5.8	17.9
w2	54.3	1.50	55.2	5.4	9.9	10.5
w4	57.2	0.25	81.5	7.8	11.0	9.4
w8	56.9	0.18	90.7	10.1	17.6	5.9
w8a2	25.4	0.18	94.5	15.6	26.9	3.9
w8ba	1.6	0.18	135.4	21.9	34.7	3.0

[a] Obtained by the mass difference of precipitate before and after drying/the mass of precipitate before drying × 100%.
[b] Sodium content of the as-prepared catalyst determined by ICP-AES.
[c] S_{BET} of the as-prepared catalyst calculated by BET method.
[d] Determined by N_2O chemisorption.
[e] Calculated by the equation of 6000/(8.92 × S_{Cu}/Cu fraction in 1 g catalyst) reported by reference [19].

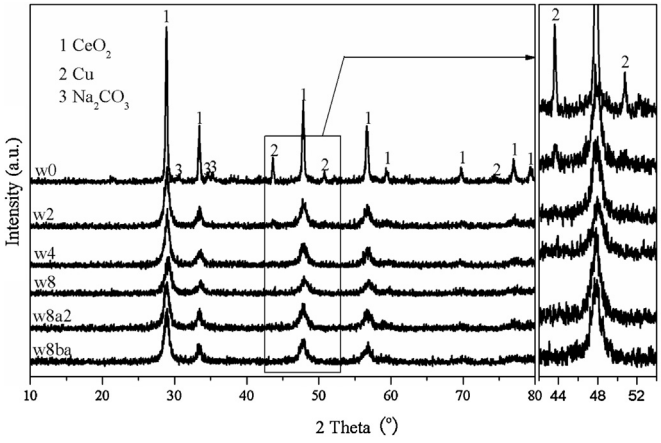

Fig. 3. XRD patterns of the fresh Cu-CeO_2-Al_2O_3 catalysts.

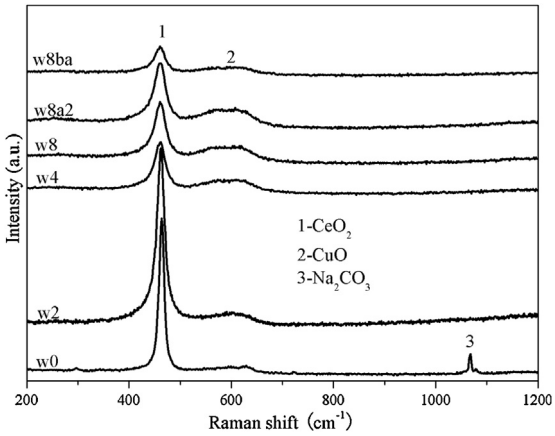

Fig. 4. Raman spectra of the as-prepared Cu-CeO_2-Al_2O_3 catalysts.

w0 and w2 catalysts, indicating that small CuO crystallites were formed and highly dispersed in the as-prepared w4, w8, w8a2 and w8ba catalysts with the relatively low contents of sodium and water in the catalyst precursors. Such observations are consistent with the results reported in the literature [19,20], in which the presence of sodium led to growth of the crystalline grain of some constituents in the catalyst. The characteristic diffraction peaks of Na_2CO_3 (PDF# 49-1816) were only observed in the as-prepared w0 catalyst, indicating that sodium existed in the form of Na_2CO_3 in the as-prepared w0 catalyst. The embedment of the precipitating agent in the as-prepared precipitate was likely a source of Na_2CO_3 in Cu-CeO_2-Al_2O_3 catalysts.

Fig. 3 shows XRD patterns of the fresh Cu-CeO_2-Al_2O_3 catalysts with different contents of sodium and water in the catalyst precursors, which were prepared by reduction of the as-prepared Cu-CeO_2-Al_2O_3 catalysts before evaluation of their catalytic performances. Compared with XRD patterns of the as-prepared Cu-CeO_2-Al_2O_3 catalysts shown in Fig. 2, the characteristic diffraction peaks of CeO_2 and Na_2CO_3 did not change after reduction of the as-prepared Cu-CeO_2-Al_2O_3 catalysts, but the characteristic diffraction peaks of CuO in the as-prepared w0 and w2 catalysts disappeared and the characteristic diffraction peaks of metallic Cu appeared at the same time, indicating that CuO was completely reduced into metallic Cu under the reduction conditions in this work. However, the characteristic diffraction peaks of metallic Cu were not observed in the fresh w4, w8, w8a2 and w8ba catalysts, indicating that small metal Cu crystallites were formed in these fresh catalysts and could be related with a high metal Cu dispersion.

3.2.2. Raman spectroscopy

Fig. 4 shows Raman spectra of the as-prepared Cu-CeO_2-Al_2O_3 catalysts with different contents of sodium and water in the catalyst precursors. The absorption bands at 466 cm^{-1} and 615 cm^{-1} were assigned to vibration modes of the F_{2g} mode of CeO_2 [28,29] and the B_g mode of CuO, respectively. With a decrease in the contents of the residual sodium and water in the catalyst precursors, the two absorption bands were broadened, which indicated a decrease in the corresponding grain sizes [30,31] and thus agreed well with the results determined from XRD and N_2O chemisorption. The absorption band at 1077 cm^{-1} assigned to the symmetric stretching mode of CO_3^{2-} [32,33] appeared in the Na-rich w0 catalyst, which further indicated that sodium existed in the form of Na_2CO_3.

3.2.3. SEM

SEM images of the as-prepared Cu-CeO_2-Al_2O_3 catalysts are shown in Fig. 5. The as-prepared w0 catalyst displayed a compact surface, ascribed to sintering of the support matrix induced by the residual sodium and the coverage of Na_2CO_3 on the surface. With a decrease in the sodium content, the as-prepared w8 catalyst showed the morphology of agglomeration of the corresponding matrix particles. On the other hand, with a decrease in the water content in the catalyst precursors, the agglomeration degree of the as-prepared Cu-CeO_2-Al_2O_3 catalysts gradually decreased, and the separated small particles or flakes appeared in the as-prepared w8a2 catalyst and the loose and feather-like species appeared in the as-prepared w8ba catalyst. Therefore the residual sodium and water in the catalyst precursors can influence thermal treatment of the catalyst precursors, which results in the different morphology and specific surface areas (S_{BET}) of the as-prepared Cu-CeO_2-Al_2O_3 catalysts.

3.2.4. Nitrogen sorption and N_2O chemisorption

Table 1 shows the physiochemical properties of Cu-CeO_2-Al_2O_3 catalysts. As shown in Table 1, the specific surface area (S_{BET}) of the as-prepared Cu-CeO_2-Al_2O_3 catalyst gradually increased from 13.5 to 90.7 $m^2\,g^{-1}$ with a decrease in the sodium content from 6.20 to 0.18 wt.% due to a decrease in sintering of the support matrix induced by sodium and plugging of the catalyst pores by Na_2CO_3 [19,34]. With further removal of the residual water in the catalyst precursors by ethanol washing or azeotropy distillation, S_{BET} of the as-prepared w8a2 and w8ba catalysts increased further. This is because the serious capillary effect of the residual water can result in sintering of the support matrix due to pore collapse. On the other hand, with a decrease in the contents of the residual sodium and water in the catalyst precursors, Cu dispersion and Cu surface area (S_{Cu}) increased in the fresh Cu-CeO_2-Al_2O_3 catalysts, that is to say, there were more active sites of Cu^0 species created on the surface of the fresh Cu-CeO_2-Al_2O_3 catalysts. It is generally considered that Cu^0 species are the active sites of Cu-based catalysts for GHMG [11–13,35]. Combined Fig. 1 with Table 1, higher Cu dispersion and Cu surface area are beneficial to increase the catalytic activity, selectivity to GBL and stability of the fresh Cu-CeO_2-Al_2O_3 catalysts, which agrees well with the results reported by our previous work [15].

3.2.5. H_2-TPR

Fig. 6 shows H_2-TPR profiles of the as-prepared Cu-CeO_2-Al_2O_3 catalysts. As shown in Fig. 6, the H_2-TPR behaviors of the as-prepared Cu-CeO_2-Al_2O_3 catalysts were significantly influenced by the contents of sodium and water in the catalyst precursors. The H_2-TPR profiles of w0, w2 and w4 catalysts showed two reduction peaks in the temperature range of 300–500 °C. The low-temperature peaks of reduction located at 358–382 °C in w0, w2 and w4 catalysts were attributed to reduction of slightly interacting

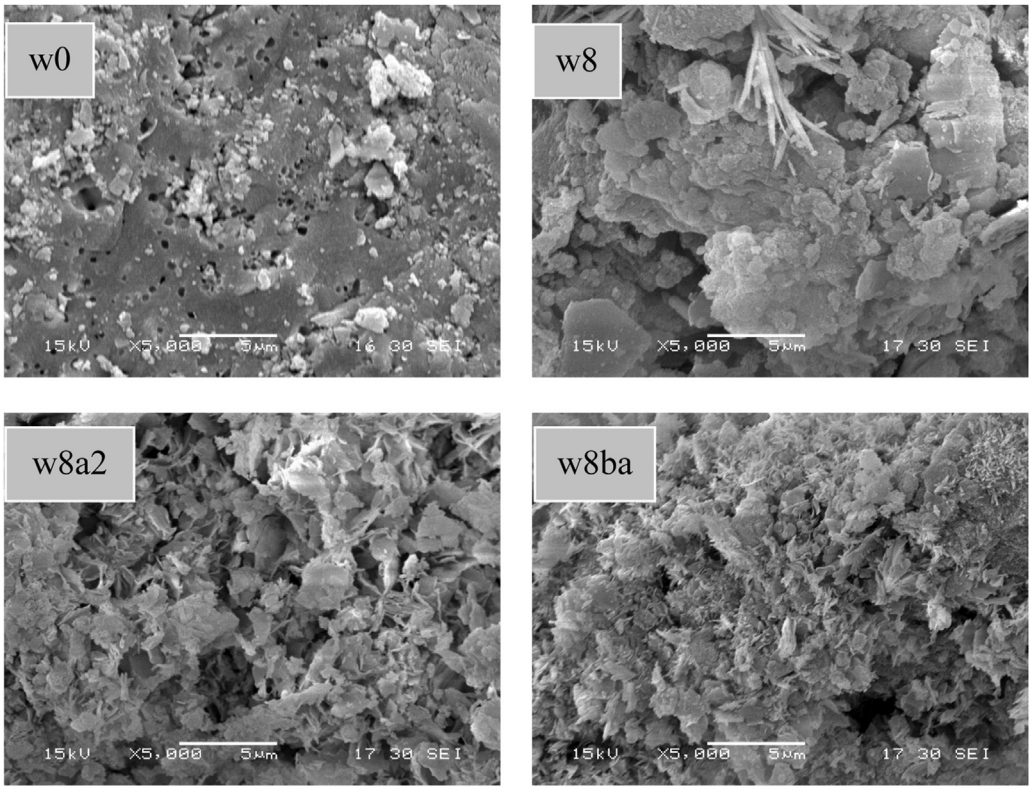

Fig. 5. SEM images of the as-prepared Cu-CeO_2-Al_2O_3 catalysts.

CuO species and the high-temperature peaks of reduction located at 431–445 °C were attributed to reduction of strongly interacting CuO species with sodium [36,37]. With a decrease in the sodium content in the catalyst precursors, the area of the high-temperature peak of reduction gradually reduced and the reduction temperature shifted to lower temperature, while the area of the low-temperature peak of reduction increased and the reduction temperature shifted to higher temperature. With a decrease in the sodium content, the reducibility of the as-prepared Cu-CeO_2-Al_2O_3 catalysts strengthened and followed an order of w4 > w2 > w0. As for w8, w8a2 and w8ba catalysts, only a reduction peak was observed and the peak temperature gradually decreased in an order of w8 > w8a2 > w8ba, which indicated that the residual water in the catalyst precursors also brought much negative effects on the reducibility of the as-prepared Cu-CeO_2-Al_2O_3 catalysts. These results indicate that high dispersion and small particle size of CuO crystallite are beneficial to its reduction.

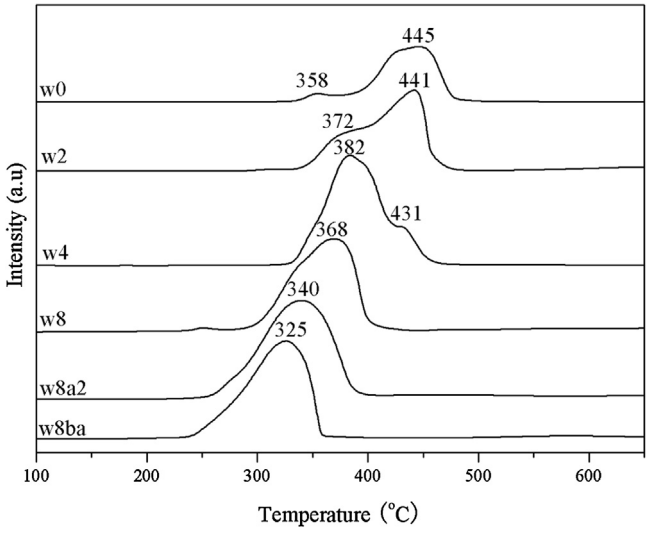

Fig. 6. H_2-TPR profiles of the as-prepared Cu-CeO_2-Al_2O_3 catalysts.

4. Conclusions

Effects of the residual sodium and water in the catalyst precursor on the catalytic performance of Cu-CeO_2-Al_2O_3 catalyst, prepared by co-precipitation method, were investigated for gas-phase hydrogenation of maleic anhydride to γ-butyrolactone at atmospheric pressure. The results show that the residual sodium and water in the catalyst precursor are unfavorable to the catalytic performance and the stability of Cu-CeO_2-Al_2O_3 catalyst. The residual sodium and water in the catalyst precursor result in the serious sintering of the as-prepared Cu-CeO_2-Al_2O_3 catalyst during thermal treatment of the catalyst precursor. As a result, with a decrease in the contents of the residual sodium and water in the catalyst precursor, the specific surface area of the as-prepared Cu-CeO_2-Al_2O_3 catalyst, S_{Cu} and Cu dispersion of the fresh Cu-CeO_2-Al_2O_3 catalyst increase. Since Cu^0 species are the active sites of Cu-based catalyst for GHMG, high Cu dispersion and S_{Cu} of the fresh Cu-CeO_2-Al_2O_3 catalyst certainly result in higher catalytic performance and stability. The residual sodium in the form of Na_2CO_3 in the as-prepared Cu-CeO_2-Al_2O_3 catalyst covers the active sites on the catalyst surface and consequently decreases the catalytic performance of Cu-CeO_2-Al_2O_3 catalyst. These results are significant to further improve the catalytic performance and stability of Cu-CeO_2-Al_2O_3 catalyst for GHMG.

Acknowledgements

This project was supported by National Basic Research Program of China (2010CB732300, 2013CB933201), Program for New

Century Excellent Talents in University (NCET-09-0343), Shu Guang Project of Shanghai Municipal Education Commission and Shanghai Education Development Foundation (10SG30).

References

[1] Y.S. Yoon, H.K. Shin, B.S. Kwak, Catal. Commun. 3 (2002) 349–355.
[2] Y. Shimasaki, H. Yano, H. Sugiura, H. Kambe, Bull. Chem. Soc. Jpn. 81 (2008) 449–459.
[3] J.Y. Huang, X.J. Liu, X.L. Kang, Z.X. Yu, T.T. Xu, W.H. Qiu, J. Power Sources 189 (2009) 458–461.
[4] S.S. Zhang, D. Foster, J. Read, J. Power Sources 188 (2009) 532–537.
[5] S.M. Jung, E. Godard, S.Y. Jung, K.C. Park, J.U. Choi, Catal. Today 87 (2003) 171–177.
[6] S.M. Jung, E. Godard, S.Y. Jung, K.C. Park, J.U. Choi, J. Mol. Catal. A: Chem. 198 (2003) 297–302.
[7] Q. Wang, H.Y. Cheng, R.X. Liu, J.M. Hao, Y.C. Yu, F.Y. Zhao, Catal. Today 148 (2009) 368–372.
[8] M. Messori, A. Vaccari, J. Catal. 150 (1994) 177–185.
[9] G.L. Castiglioni, A. Vaccari, G. Fierro, M. Inversi, M.L. Jacono, G. Minelli, I. Pettiti, P. Porta, M. Gazzano, Appl. Catal. A: Gen. 123 (1995) 123–144.
[10] G.L. Castiglioni, M. Ferrari, A. Guercio, A. Vaccari, R. Lancia, C. Fumagalli, Catal. Today 27 (1996) 181–186.
[11] T.J. Hu, H.B. Yin, R.C. Zhang, H.X. Wu, T.S. Jiang, Y.J. Wada, Catal. Commun. 8 (2007) 193–199.
[12] D.Z. Zhang, H.B. Yin, R.C. Zhang, J.J. Xue, T.S. Jiang, Catal. Lett. 122 (2008) 176–182.
[13] D.Z. Zhang, H.B. Yin, C. Ge, J.J. Xue, T.S. Jiang, L.B. Yu, Y.T. Shen, J. Ind. Eng. Chem. 15 (2009) 537–543.
[14] Y. Yu, Y.L. Guo, W.C. Zhan, Y. Guo, Y.S. Wang, G.Z. Lu, J. Mol. Catal. A: Chem. 392 (2014) 1–7.
[15] Y. Yu, Y.L. Guo, W.C. Zhan, Y. Guo, Y.Q. Wang, Y.S. Wang, Z.G. Zhang, G.Z. Lu, J. Mol. Catal. A: Chem. 337 (2011) 77–81.
[16] C.I. Meyer, S.A. Regenhardt, A.J. Marchi, T.F. Garetto, Appl. Catal. A: Gen. 417–418 (2012) 59–65.
[17] S.A. Regenhardt, C.I. Meyer, T.F. Garetto, A.J. Marchi, Appl. Catal. A: Gen. 449 (2012) 81–87.
[18] C.I. Meyer, S.A. Regenhardt, M.E. Bertone, A.J. Marchi, T.F. Garetto, Catal. Lett. 143 (2013) 1067–1073.
[19] K.W. Jun, W.J. Shen, K.S. Rama Rao, K.W. Lee, Appl. Catal. A: Gen. 174 (1998) 231–238.
[20] Z.W. Huang, F. Cui, H.X. Kang, J. Chen, C.G. Xia, Appl. Catal. A: Gen. 366 (2009) 288–298.
[21] A.X. Hao, Y. Yu, H.B. Chen, C.P. Mao, S.X. Wei, Y.S. Yin, Acta Phys. Chim. Sin. 29 (2013) 2047–2055.
[22] H.B. Shan, Z.T. Zhang, J. Eur. Ceram. Soc. 17 (1997) 713–717.
[23] Y.V. Kolen'ko, A.V. Garshev, B.R. Churagulov, S. Boujday, P. Portes, C.C. Justin, J. Photochem. Photobiol. A: Chem. 172 (2005) 19–26.
[24] Q. Wang, G.F. Li, B. Zhao, R.X. Zhou, Appl. Catal. B: Environ. 100 (2010) 516–528.
[25] M. Chen, P.H. Zhang, X.M. Zheng, Catal. Today 93–94 (2004) 671–674.
[26] S.S. Prakash, C.J. Brinker, A.J. Hurd, S.M. Rao, Nature 374 (1995) 439–443.
[27] X.M. Guo, D.S. Mao, S. Wang, G.S. Wu, G.Z. Lu, Catal. Commun. 10 (2009) 1661–1664.
[28] G.W. Graham, W.H. Weber, C.R. Peters, R. Usmen, J. Catal. 130 (1991) 310–313.
[29] Z.Q. Yang, D.S. Mao, X.M. Guo, G.Z. Lu, J. Rare Earths 32 (2014) 117–123.
[30] J. Zuo, C.Y. Xu, Y.P. Liu, Y.T. Qian, Nanostruct. Mater. 10 (1998) 1331–1335.
[31] L. Ilieva, G. Pantaleo, I. Ivanov, A.M. Venezia, D. Andreeva, Appl. Catal. B: Environ. 65 (2006) 101–109.
[32] J. Wu, H.F. Zhang, Chem. Geol. 273 (2010) 267–271.
[33] J.F. Widmann, C.L. Aardahl, E.J. Davis, Trends Anal. Chem. 17 (1998) 339–345.
[34] K.V.R. Chary, G.V. Sagar, D. Naresh, K.K. Seela, B. Sridhar, J. Phys. Chem. B 109 (2005) 9437–9444.
[35] Y.L. Zhu, H. Yang, G.Q. Dong, H.Y. Zheng, H.H. Zhang, H.W. Xiang, Y.W. Li, Appl. Catal. B: Environ. 57 (2005) 183–190.
[36] G. Díaz, R. Pérez-Hernández, A. Gómez-Cortés, M. Benaissa, R. Mariscal, J.L.G. Fierro, J. Catal. 187 (1999) 1–14.
[37] F.W. Chang, H.C. Yang, L.S. Roselin, W.Y. Kuo, Appl. Catal. A: Gen. 304 (2006) 30–39.